Bioorg. Med. Chem. 46 (2021) 116390

Contents lists available at ScienceDirect

Bioorganic & Medicinal Chemistry

journal homepage: www.elsevier.com/locate/bmc

Synthesis, in vitro cytotoxicity and biological evaluation of twenty novel 1,3-benzenedisulfonyl piperazines as antiplatelet agents

Xiu-jie Liu [a,b,*], Yan Wang [a,c], Xiao Wang [a], Zhi-hao Zhang [d,*]

[a] School of Chemistry and Chemical Engineering, Tianjin University of Technology, 300384 Tianjin, China
[b] Tianjin Key Laboratory of Drug Targeting and Bioimaging, Tianjin Key Laboratory of Organic Solar Cells and Photochemical Conversion, School of Chemistry and Chemical Engineering, Tianjin University of Technology, 300384 Tianjin, China
[c] Asymchem Laboratories (Tianjin) Co., Ltd., Tianjin 300457, China
[d] School of Pharmacy, Nanjing Medical University, Nanjing 211166, China

ARTICLE INFO

Keywords:
N^1,N^3-dipiperazinyl-4-methoxy(ethoxy)-1,3-benzenedisulfonamide
Synthesis
In vitro anti-platelet activity
Cytotoxicity
Docking studies
In silico ADME prediction

ABSTRACT

In order to discover antiplatelet drug with novel structure and expand our research scope, total twenty 1,3-benzenedisulfonyl piperazines, were designed and synthesized. These target compounds were divided into two series, namely 4-methoxy-1,3-benzenedisulfonyl piperazines of series **1** and 4-ethoxy-1,3-benzenedisulfonyl piperazines of series **2**. With adenosine diphosphate (ADP), arachidonic acid (AA) and collagen as inducers, respectively, the Born turbidimetric method was used to screen the antiplatelet activity in vitro of all target compounds at a concentration of 1.3 μM, with aspirin and picotamide as positive control drugs. And of which, the activities of five compounds for collagen were higher than both picotamide and aspirin. In ADP or AA channel, compounds with an inhibition rate greater than 33% were selected, and their corresponding IC_{50} values were obtained. According to the IC_{50}, the in vitro activity of one compound for ADP was higher than picotamide, and for AA, two compounds were higher than two positive control drugs and other two compounds only higher than or equal to aspirin. The preliminary analysis of the structure-activity relationship of the target compounds involved in this study was completed. Further, eight compounds exhibiting higher activity in one or two test channels, were subjected to cytotoxicity test on mouse fibroblasts (L929) by CCK-8 method. The in vitro cytotoxicity of most test compounds showed less than or same to control drug picotamide at 10 μM, but at the higher concentration of 100 μM, merely two compounds exhibited higher cell survival rate than that of picotamide. In addition, compound N^1,N^3-di(4-ethoxy-1,3-phenylenedisulfonyl)bis(1-(*m*-tolyl)piperazine), which is delivery activity in the three test channels, and another compound N^1,N^3–di(4-methoxy-1,3-phenylenedisulfonyl)bis(1-(*m*-tolyl)piperazine), which has the lowest cytotoxic in vitro compound among series **1** and series **2**, respectively, are found and selected for simulation analysis as two most likely to dock with the receptor P_2Y_{12}. Each of synthesized compounds in silico molecular property and ADME (absorption, distribution, metabolism and excretion) are predicted by using Molinspiration property engine v2018.10 and PreADMET online servers, respectively. Compared with other series of compounds in the previous stage, the two series compounds obtained after the introduction of piperazinyl have a similar in vitro activity.

1. Introduction

With the acceleration of economic development and people's lives, the prevalence and mortality of thrombotic diseases have been increasing.[1–3] Among them, platelet is a key participant in atherothrombosis.[4] Antiplatelet drugs occupy an important position in the treatment of thrombotic diseases. So, the development of new antiplatelet drug with higher activity, lower toxicity, and broader effects has extremely high social & economic significance.[5]

Picotamide (Fig. 1), as an anti-platelet aggregation drug, has a certain broad spectrum and multiple mechanisms of action.[6] The clinical comparison studies in recent years have shown that picotamide significantly surpasses aspirin in the treatment of atherosclerosis and the treatment of thrombosis in diabetic patients with cardiac and

* Corresponding authors at: School of Chemistry and Chemical Engineering, Tianjin University of Technology, 300384 Tianjin, China (X.-J. Liu); School of Pharmacy, Nanjing Medical University, 211166 Nanjing, China (Z.-H. Zhang).
E-mail addresses: liuxiujiechem@163.com (X.-j. Liu), zhangzhihaochem@163.com (Z.-h. Zhang).

https://doi.org/10.1016/j.bmc.2021.116390
Received 13 June 2021; Received in revised form 23 August 2021; Accepted 25 August 2021
Available online 30 August 2021

cerebrovascular complications.[7,8] Relevant departments in many countries pay more attention to and strengthen the research and development of picotamide itself and its structural modification work,[9–12] and 2NTX-99 is one of the most successful.[13] The piperazines has always been a type of substituent that often appear in drug structure, which could usually increase the water solubility of the drug, thereby improving the bioavailability of the drug.[14,15]

Since 1999, by replacing two pyridine groups connected to the two side chains at the 1,3-position of picotamide structure with two substituted phenyl groups, our research group began to design and synthesize novel structural analogs of picotamide.[16–19] After screening the in vitro antiplatelet activity of nearly one hundred 4-methoxy-1,3-phthaloyl compounds obtained, it was found that eighteen compounds had higher activity than that of picotamide. Next, according to the isostere theory and similar research on a larger scale, substituting sulfonyl for acyl, and further substituting 4-ethoxy for methoxy, two new series of 4-methoxy-1,3-benzenedisulfonamides (Fig. 1) and 4-ethoxy-1,3-benzenedisulfonamides (Fig. 1) were prepared.[20,21] Compared with the amide compounds prepared in the early stage, the sulfonamide compounds developed in the later stage with lower synthesis cost and better water solubility, which allows more choices of solvents for recrystallization and subsequent pharmacological research, and so that new compounds with higher activity in almost the same proportions were discovered.

In order to discover antiplatelet drugs with novel structures and expand our research scope, this paper used piperazine groups with better water solubility and higher polarity to replace the anilines, total twenty 1,3-benzenedisulfonyl bis(1-hydrocarbyl piperazines), were designed and synthesized, and were divided into two series, namely 4-methoxy-1,3-benzenedisulfonyl bis(1-hydrocarbyl piperazine) of series **1** (**7a-j**) and 4-ethoxy-1,3-benzenedisulfonyl bis(1-hydrocarbyl piperazine) of series **2** (**10a-j**). The chemical structures of each target compounds have been confirmed by ^{1}H NMR, ^{13}C NMR, IR and ESI-MS. The design idea and corresponding structures of target compounds were given in Fig. 1. With adenosine diphosphate (ADP), arachidonic acid (AA) or collagen as an inducer, respectively, two clinically mature antiplatelet drugs aspirin and picotamide were selected as positive control drugs, and at the concentration of 1.3 μM, the Born turbidimetric method was used to screen the anti-platelet activity in vitro of compounds **7a-j** and **10a-j**. Eight compounds **7a**, **7e**, **7f**, **7i**, **10e**, **10f**, **10i** and **10j** exhibiting high antiplatelet activity in one or two test channels, were subjected to cytotoxicity test on mouse fibroblasts (L929) by CCK-8 method. In addition, **7i** and **10i,** as representatives of series **1** and series **2**, respectively, were selected for simulation analysis as two most likely to dock with the receptor P_2Y_{12}. Each of synthesized compounds in silico molecular property and ADME (absorption, distribution, metabolism and excretion) were predicted by using Molinspiration property engine v2018.10 and PreADMET online servers, respectively.

2. Results and discussion

2.1. Chemistry

One kind of the key intermediates for the synthesis of target compounds are different *N*-hydrocarbyl substituted piperazines **4a-j**. Among them, the synthetic pathway of the **4h-j** self-synthesized was depicted in Scheme 1. Using bis(2-hydroxyethyl)amine (**1**) as the starting material, react firstly with $SOCl_2$ to produce bis(2-chloroethylamine) hydrochloride (**2**), and then continue to undergo two amination reactions with different aromatic amines (**3h–j**) to produce the key intermediate *N*-hydrocarbyl substituted piperazines (**4h-j**) according to design needs: *N*-(2-methylphenyl)piperazine (**4h**, yield: 31.26%), *N*-(3-methylphenyl)piperazine (**4i**, yield: 33.14%) and *N*-(4-methylphenyl) piperazine (**4j**, yield: 71.90%). while other substituted piperazines **4a-g** used were commercially available.

Two synthetic routes and the structures of target compounds **7a-j** of series **1** and **10a-j** of series **2** are listed in the Scheme 2. Regarding the synthetic route of target compounds **7a-j** of series **1**, using anisole (**5**) as starting material, react with chlorosulfonic acid and thionylchide to produce intermediate 4-methoxybenzene-1,3-disulfonyl chloride (**6**) in dichloromethane, continued with different *N*-hydrocarbyl piperidines and undergo amination reaction in tetrahydrofuran to generate the target compounds **7a-j**.

In addition to different one starting material phenethyl ether (**8**), the synthetic method of target compounds **10a-j** of series **2**, is similar to series **1**. With phenethyl ether (**8**) as the starting material, 4-ethoxy-1,3-phthaloyl chloride (**9**) is generated by the reaction of chlorosulfonylation, and then, the target compounds **10a-j** are generated by the reaction (**9**) of amination with different *N*-hydrocarbyl substituted piperazines **4a-j**.

Compared with the compounds obtained by introducing the phenyl group in the previous stage, the water solubility of the compound synthesized by introducing the piperazine group in this study has been improved, so that the number of solvents that can be used for recrystallization is increased.

2.2. Biological assays

2.2.1. Evaluation of in vitro anti-platelet aggregation activity

After the target compounds are prepared, purified and structure determined, the Born turbidimetric method[22,23] is used to screen their antiplatelet aggregation activity in vitro with ADP, AA or collagen as an inducer, respectively. Of which, the determination of collagen channel is limited to the study of the aggregation rate only at the concentration of

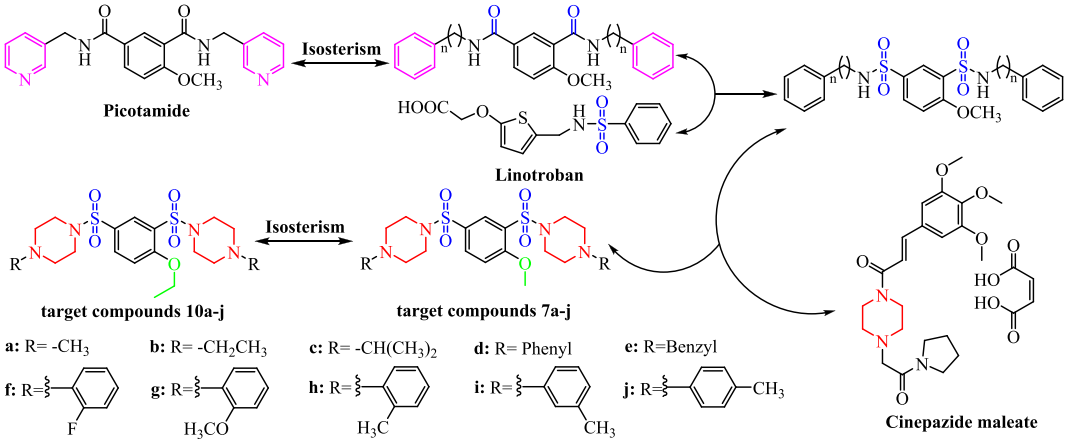

Fig. 1. Structure of picotamide and target compounds & the design idea.

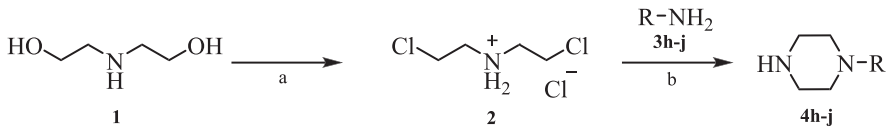

Reagents and conditions: (a) $SOCl_2$, CH_2Cl_2, 5h, r.t. (b) $CH_3(CH_2)_3OH$, Na_2CO_3, 130 °C, 48h

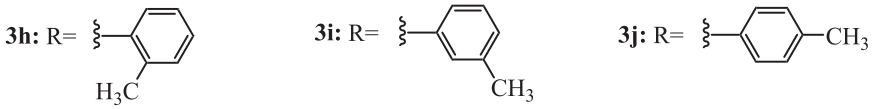

Scheme 1. Synthetic routes to intermediates of *N*-hydrocarbyl piperazines **4h-j.**

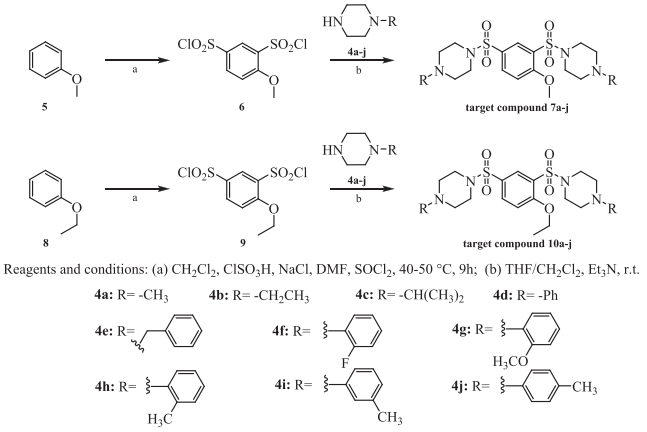

Scheme 2. Synthetic routes and structures of target compounds **7a-j** of series **1** and **10a-j** of series **2.**

1.3 μM. Through conversion, the corresponding inhibition rate is obtained. Among them, seven compounds with over 33% inhibition rate in AA test channel and eight compounds with over 33% inhibition rate in ADP test channel, respectively, and their corresponding IC_{50} values are also obtained by calculation. And the positive drugs are picotamide and aspirin.

In vitro anti-platelet aggregation activities of target compounds are measured using rabbit venous blood. Fresh venous blood is taken from the ear vein of rabbits (weight: 2–3 kg, male), with 3.8% sodium citrate as anticoagulant (9:1 by volume). Samples are centrifuged at 1000 rpm/min for 10 min at room temperature to obtain the platelet-rich plasma (PRP). The PRP supernatant is removed and the residue is centrifuged at 3000 rpm/min for 10 min at room temperature to obtain platelet-poor plasma (PPP), which is used as the blank. Target compounds (1.3 μM) are previously dissolved in dimethylsulfoxide (DMSO), and the solution (5 μL) is added into PRP (200 μL) and incubated for 2 min. Aggregation is induced by adding 20 μL ADP (5 mM), collagen (1 mg/mL) or AA (20 μM), repectively. DMSO (0.5% v/v) is used as negative control (according to the pre-experiment, 5 μL DMSO showed no significant effect on the platelet aggregation), and picotamide and aspirin are used as standard drugs. When the inducer used is ADP or AA, the compounds which have higher anti-platelet aggregation activity at the concentration of 1.3 μM are diluted to 0.65 μM and 0.325 μM, and then repeat the same operation and calculation method to get the corresponding IC_{50} value. The platelet aggregation inhibition rate (%) are calculated according to the following formula:

$$Inhibition\% = (1 - D/S) \times 100\%$$

where D = platelet aggregation in the presence of test compounds, S = platelet aggregation in the presence of solvent. The primary screening data for all compounds (1.3 μM) in vitro activity on antiplatelet aggregation of the synthesized compounds are given in Table 1. The Statistical analysis is performed with ANOVA followed by Tukey's test. In the ADP and AA channels, target compounds with an inhibition rate greater than 33% are selected, corresponding IC_{50} values are also given in Table 1.

Table 1
Anti-platelet aggregation activity in vitro data of compounds.

Compd.	Inhibition rate/% (ADP)	IC_{50}/(μM) (ADP)	Inhibition rate/% (AA)	IC_{50}/(μM) (AA)	Inhibition rate/% (collagen)
7a	38.19% ± 0.03$^{**\#\#}$	0.98	29.52% ± 0.14**		52.63% ± 0.17
7b	24.27% ± 0.09$^{*\#}$		22.41% ± 0.04**		42.64% ± 0.13$^{**\#\#}$
7c	28.38% ± 0.12$^{*\#}$		27.07% ± 0.04**		49.42% ± 0.11$^{**\#}$
7d	27.91% ± 0.22$^{**\#\#}$		15.67% ± 0.06**		20.41% ± 0.07
7e	33.21% ± 0.07$^{**\#\#}$	1.15	38.46% ± 0.13	0.33	22.79% ± 0.07
7f	27.97% ± 0.08$^{*\#}$		40.64% ± 0.11**	0.48	28.81% ± 0.14$^{**\#\#}$
7g	28.74% ± 0.11$^{**\#\#}$		28.15% ± 0.13**		27.59% ± 0.13$^{**\#\#}$
7h	38.94% ± 0.12$^{**\#\#}$	0.95	36.88% ± 0.08	0.36	32.13% ± 0.09$^{**\#\#}$
7i	21.06% ± 0.06$^{**\#\#}$		33.74% ± 0.06**	0.71	54.24% ± 0.16$^{**\#\#}$
7j	30.37% ± 0.14$^{**\#\#}$		34.14% ± 0.09**	0.68	32.61% ± 0.08$^{**\#\#}$
10a	24.48% ± 0.05$^{**\#\#}$		18.12% ± 0.05**		29.53% ± 0.11$^{**\#}$
10b	28.84% ± 0.1$^{*\#\#}$		29.90% ± 0.06**		41.70% ± 0.17$^{**\#\#}$
10c	36.38% ± 0.1$^{*\#}$	0.80	24.93% ± 0.12**		39.05% ± 0.11$^{**\#\#}$
10d	40.07% ± 0.14$^{*\#}$	0.91	23.61% ± 0.07*		26.95% ± 0.06$^{*\#}$
10e	24.00% ± 0.08$^{**\#}$		20.14% ± 0.10**		49.76% ± 0.12$^{**\#\#}$
10f	21.02% ± 0.08$^{*\#}$		25.81% ± 0.14**		50.28% ± 0.07$^{**\#\#}$
10g	25.52% ± 0.11$^{**\#\#}$		23.08% ± 0.13**		25.25% ± 0.07$^{**\#\#}$
10h	28.94% ± 0.14$^{*\#}$		33.08% ± 0.14*	0.65	41.59% ± 0.06$^{**\#\#}$
10i	50.27% ± 0.06$^{*\#}$	0.45	34.84% ± 0.15*	0.43	48.79% ± 0.07$^{**\#\#}$
10j	43.61% ± 0.11$^{*\#\#}$	0.72	42.98% ± 0.09	0.26	28.50% ± 0.07$^{**\#\#}$
Picotamide	45.49% ± 0.12	0.47	37.08% ± 0.16	0.34	49.17% ± 0.13
Aspirin	46.30% ± 0.06	0.44	38.45% ± 0.13	0.43	49.12% ± 0.18

* $\rho < 0.05$ versus control, ** $\rho < 0.01$ versus control.
$^{\#}$ $\rho < 0.05$ versus picotamide, $^{\#\#}$ $\rho < 0.01$ versus picotamide.

1. As illustrated in Table 1 and Fig. 2 for the platelet aggregation induced by ADP, the order of the target compounds with obvious anti-platelet activity of series **2** at the concentration of 1.3 μM is: **10i** (50.27%) > aspirin (46.30%) > picotamide (45.49%) > **10j** (43.61%) > **10d** (40.07%) > **10c** (36.38%). Among them, the inhibition rate of

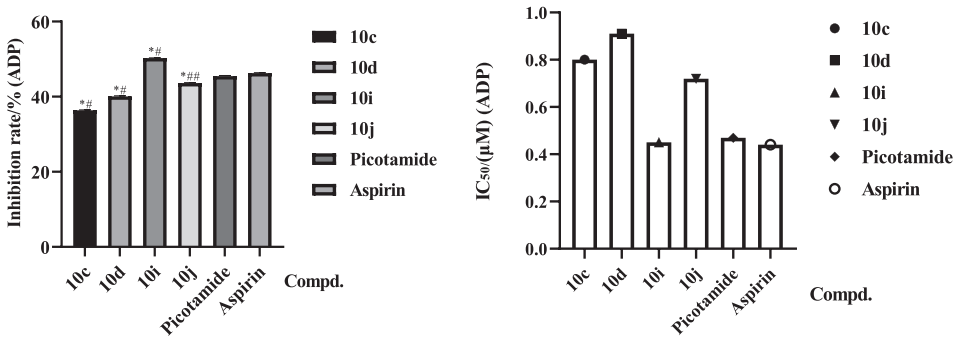

Fig. 2. The inhibition rate and IC_{50} of some target compounds of series **2** for ADP.

compound **10i** is the highest. The order of the calculated IC_{50} values of four potent compounds is: **10d** (0.91 μM) > **10c** (0.80 μM) > **10j** (0.72 μM) > picotamide (0.47 μM) > **10i** (0.45 μM) > aspirin (0.44 μM). There is a compound **10i** with IC_{50} values lower than picotamide. The order of the corresponding structure and activity relationship thus obtained is: **10i** (*N*-3-CH_3 Phenyl) > **10j** (*N*-4-CH_3 Phenyl) > **10c** (*N*-$CH(CH_3)_2$) > **10d** (*N*-Phenyl).

From the structural point of view, compound **10i**, that is N^1,N^3-di(4-ethoxy-1,3-phenylenedisulfonyl)bis(1-(*m*-tolyl)piperazine), in which introducing a 3-methylphenyl group at the 4-position *N* of the two side chain piperazine rings, respectively. At this point, it seems that increasing the steric hindrance of *N*-substituents could increase the anti-platelet aggregation activity of target compounds. When a methyl phenyl group is introduced into the 4-position *N* of two side chain piperazine rings, the 3-position methyl group is more advantageous. The in vitro activity order of the obtained methyl groups at different positions is: **10i** (3-CH_3) > **10j** (4-CH_3) > **10h** (2-CH_3).

Obviously, the compounds **10a-j** of series **2** with 4-ethoxy structure are generally stronger than the compounds **7a-j** series **1** with 4-methoxy structure in terms of in vitro antiplatelet activity. And in the latter, no compound can reach or approach the inhibition rate of picotamide. Since the in vitro antiplatelet activity of series **1** is generally low, the structure–activity relationship has not been discussed here.

2. For AA-induced platelet aggregation, based on the data of Table 1 and Fig. 3, three compounds **7e**, **7f** and **10j** showed higher inhibitory activity on platelet aggregation than both picotamide and aspirin. The order of the corresponding inhibition rate of five main compounds and two positive control drugs at a concentration of 1.3 μM is: **10j** (42.98%) > **7f** (40.64%) > **7e** (38.46%) > aspirin (38.45%) > picotamide (37.08%) > **7h** (36.88%) > **10i** (34.84%). Their IC_{50} value calculated in descending order is: **7f** (0.48 μM) > aspirin (0.43 μM), **10i** (0.43 μM) > **7h** (0.36 μM) > picotamide (0.34 μM) > **7e** (0.33 μM) > **10j** (0.26 μM). There are two compounds **7e** and **10j** with IC_{50} values lower than or equivalent to that of picotamide. It has shown that compound **10j**, that is N^1,N^3-di(4-ethoxy-1,3-phenylenedisulfonyl)bis(1-(*p*-tolyl)piperazine), which was prepared by introducing a 4-methylphenyl group at the 4-position *N* of piperazine, has the lowest IC_{50} value and the highest in vitro antiplatelet activity among both all test compounds and positive control drugs. Further analysis the data of anti-platelet activity, the preliminary speculations on the structure–activity relationship is initially summarized as follows:

For the compound **7a-j** of series **1** where the parent benzene ring is connected to the methoxy group at the 4-position, the order of in vitro anti-platelet activity of related compounds is: **7e** (*N*-CH_2Ph) > **7a** (*N*-CH_3) > **7c** (*N*-$CH(CH_3)_2$) > **7b** (*N*-CH_2CH_3) > **7d** (*N*-Ph). It is shown that the steric hindrance of *N*-substituents has no obvious effect on the activity of the compound. When the 4-position *N* is substituted by a phenyl group, the order of activity after connecting different groups at the 2-position of the corresponding phenyl group is: **7h** (2-CH_3) > **7f** (2-F) > **7g** (2-OCH_3) > **7d** (2-H). And the order of activity after connecting the different positions of the corresponding phenyl group to the methyl group is: **7h** (2-CH_3) > **7j** (4-CH_3) > **7i** (3-CH_3), when substituent is methyl on the 2-position, the anti-platelet aggregation activity is significantly higher.

For the compound **10a-j** of series **2**, their order of in vitro activity of related compounds is: **10b** (*N*-CH_2CH_3) > **10c** (*N*-$CH(CH_3)_2$) > **10d** (*N*-Ph) > **10e** (*N*-CH_2Ph) > **10a** (*N*-CH_3), which indicates that there is no obvious law of influence of steric hindrance of *N*-substituents on the anti-platelet aggregation activity of the compound. When the *N*-substituent is phenyl, by continuing to introduce a group at the 2-position of the phenyl, the effect on the increase of platelet activity is not obvious enough, but the methyl substitution seems to be more advantageous: **10h** (2-CH_3) > **10f** (2-F) > **10d** (2-H) > **10g** (2-OCH_3). And the order of activity after connecting the different positions of the corresponding phenyl group to the methyl group is: **10j** (4-CH_3) > **10i** (3-CH_3) > **10h** (2-CH_3), that is para- position > meta- position > ortho- position.

3. According to the inhibition rate illustrated in Fig. 4 of collagen channel, the in vitro antiplatelet activities of five compounds **7a**, **7c**, **7i**, **10e** and **10f** are obviously higher than that of two control drugs and other fifteen compounds at a concentration of 1.3 μM. The order of inhibition rate of the main compounds is: **7i** (54.24%) > **7a** (52.63%) > **10f** (50.28%) > **10e** (49.76%) > **7c** (49.42%) > picotamide (49.17%) >

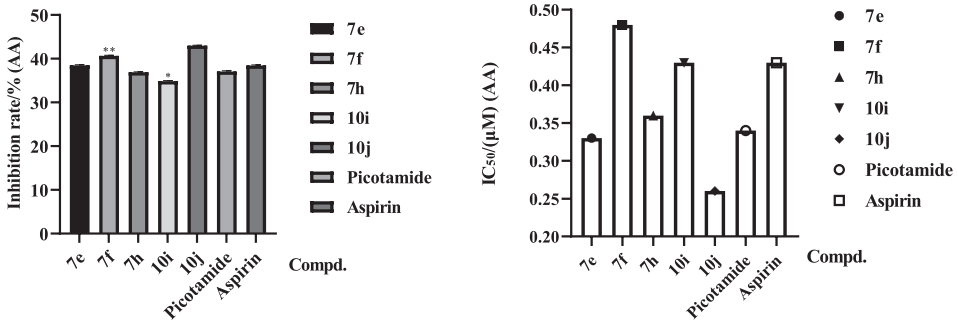

Fig. 3. The inhibition rate and IC_{50} of potent target compounds for AA.

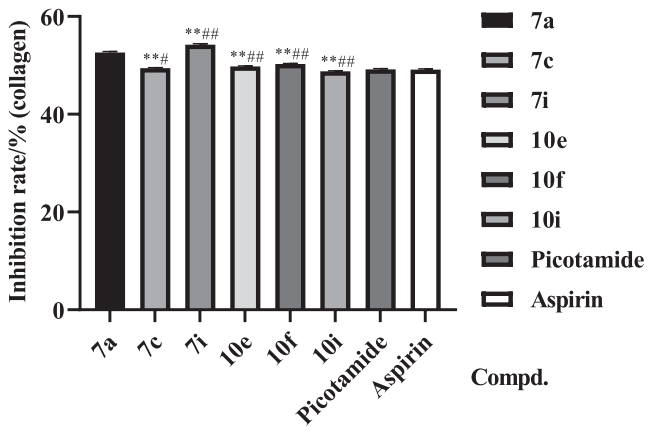

Fig. 4. The inhibition rate of potent target compounds for collagen.

aspirin (49.12%) > **10i** (48.79%). From a structural point of view, compound **7i**, that is N^1, N^3–di(4-methoxy-1,3-phenylenedisulfonyl)bis (1-(*m*-tolyl)piperazine), in which introducing a 3-methylphenyl group at the 4-position *N* of the two side chain piperazine rings, respectively, has the highest in vitro antiplatelet activity. Further analysis the data of antiplatelet activity, the preliminary speculations on the structure–activity relationship as follows:

Regarding the effect of the substituents on piperidine *N*-4 on the in vitro activity of the compound, for the compounds of series **1**, the antiplatelet aggregation activity of the compound with an aliphatic substituent is often higher than that of an aromatic substituent, and the order of in vitro activity of related compounds is: **7a** (*N*-CH_3) > **7c** (*N*-$CH(CH_3)_2$) > **7b** (*N*-CH_2CH_3) > **7e** (*N*-CH_2Ph) > **7d** (*N*-Ph). And when the *N*-substituent is phenyl, the introduction of a substituent at the 2-position of the phenyl group often could increase the activity: **7h** (2-CH_3) > **7f** (2-F) > **7g** (2-OCH_3) > **7d** (2-H).

For the compound of series **2** where the parent benzene ring is connected to the ethoxy group at the 4-position, basis on the data in Table 1, the order of in vitro activity of related compounds is: **10e** (*N*-CH_2Ph) > **10b** (*N*-CH_2CH_3) > **10c** (*N*-$CH(CH_3)_2$) > **10a** (*N*-CH_3) > **10d** (*N*-Ph). It is shown that the steric hindrance of *N*-substituents has no obvious effect on antiplatelet aggregation activity. When the *N*-substituent is phenyl, continue to introduce a substituent on this phenyl, such as methyl or fluorine at the 2-position, could increase the anti-platelet aggregation activity: **10f** (2-F) > **10h** (2-CH_3) > **10d** (2-H) > **10g** (2-OCH_3). And when the side chain phenyls' substituent is methyl, the order of activity when the methyl group is attached to different positions of the benzene ring, the order of in vitro activity is: **10i** (3-CH_3) > **10h** (2-CH_3) > **10j** (4-CH_3).

It was found in this study that compound **10i**, **10j** and **7i** have the highest in vitro platelet aggregation inhibition rate in a test channel of ADP, AA or collagen in turn, respectively.

2.2.2. Cytotoxicity test

Eight compounds **7a**, **7e**, **7f**, **7i**, **10e**, **10f**, **10i** and **10j** with lower or close to the IC_{50} value of positive control drugs aspirin and picotamide in one or two test channels of ADP, AA or collagen, are subjected to cytotoxicity in vitro test on Mouse fibroblast cells (L929) by CCK-8 method.[24,25]

Experiment is mainly divided into the following steps: L929 cells are seeded in 96-well U-bottom plates at a density of 10,000 cells per well and incubated at 37 °C for 24 h in culture medium. The cells with 100 mL of RPMI-1640 per well were allowed to attach for 24 h. Subsequently, the cells were then exposed to target compounds at a range of concentrations at 37 °C for 48 h. Target compounds concentration of 10 and 100 μM were added to L929 cells. After that, the medium was removed and replaced with 100 μM of fresh complete medium of RPMI-1640. Then, CCK-8 solution was added to the 96-well plates at 10 μM per well and incubated for a further 30 min, and the absorbance at 450 nm was measured on a microplate reader (Bio-TekFLx800 fluorescence microplate reader). Table 2 gives relative cell viability (%) relative to control wells at two concentrations tested.

The cell viability (%) is calculated by the following formula:

$$\text{Cell viability}(\%) = \text{Abs (test cell)}/\text{Abs (controlled cell)} \times 100\%;$$

As it appears in the various pictures of Fig. S1, if a test compound or a control drug has less toxic, the cells will be shuttle-shaped and adhere well, and on the contrary, the cells will be round and no longer adhere to the wall. Fig. 6 shows a comparison chart of in vitro cell viability tested at two concentrations: the darker is at 10 μM, and the lighter is at 100 μM. When the test dose is 10 μM, the cytotoxicity of seven test compounds **7a**, **7e**, **7f**, **7i**, **10e**, **10f** and **10i** are comparable or lower than that of picotamide, but when the test dose is 100 μM, only the cell survival rate of two compounds **7f** and **7i** are higher than that of picotamide. This means that at higher dose, compounds except **7f** and **7i** showed higher cytotoxicity than that of picotamide. It is found that compound **7i,** that is N^1,N^3–di(4-methoxy-1,3-phenylenedisulfonyl)bis (1-(*m*-tolyl)piperazine), has lowest in vitro cytotoxicity among both tested compounds and picotamide (see Fig. 5).

2.3. Docking studies

The crystal structure of the P_2Y_{12} receptor is obtained from the RCSB protein database (PDB code 4PXZ). The 3D structures of the two target compounds **7i** and **10i** are drawn in mol2 format by ChemBio 3D. Docking research with SYBYL, and we put the results of molecular docking in Fig 6. The "prepare protein structure" tool in the SURFLEX-DOCK module is used to repair the structure of P_2Y_{12} receptor 4PXZ, which is mainly divided into fellowing steps: Protein structure with excess water molecules deleted is used for docking simulations; Extract the ligand 2MeSADP to generate the interface bag; Add Essential hydrogen to saturate terminal amino and carboxyl groups to complete the reparation side chain amino acid residue; AMBER FF99 charge is used to describe the electrostatic characteristics. For small molecule compounds, the Tripos forcefield is used to optimize them, and the Gasteiger-Huckel charge is used to calculate the electrostatic potential. The energy convergence value and the maximum number of iterations in the optimization process are 0.005 kcal/(mol·Å) and 1,000.

In order to determine if the target compound can interact with the P_2Y_{12} receptor site on the platelet membrane, due to compound N^1,N^3-di (4-ethoxy-1,3-phenylenedisulfonyl)bis(1-(*m*-tolyl)-piperazine), which is delivery activity in the three test channels, and compound N^1,N^3–di(4-

Table 2
Cell survival rate of target compounds in vitro cytotoxicity on L929.

Compd.	Dose (μM)	Average Absorbance	Survival rate (%)
Blank	–	0.121	–
Control	–	0.130	–
Picotamide	10	0.126	55.56 ± 5.56
	100	0.125	44.44 ± 6.79
7a	10	0.128	77.78 ± 4.49
	100	0.124	33.33 ± 3.33
7e	10	0.126	55.56 ± 3.17
	100	0.123	22.22 ± 2.22
7f	10	0.128	77.78 ± 4.48
	100	0.127	66.67 ± 6.67
7i	10	0.129	85.18 ± 4.91
	100	0.127	66.67 ± 3.84
10e	10	0.126	55.56 ± 7.86
	100	0.123	22.22 ± 4.44
10f	10	0.127	70.37 ± 4.06
	100	0.121	3.70 ± 0.74
10i	10	0.126	56.56 ± 3.21
	100	0.124	33.33 ± 3.33
10j	10	0.126	51.82 ± 5.96
	100	0.122	7.40 ± 0.74

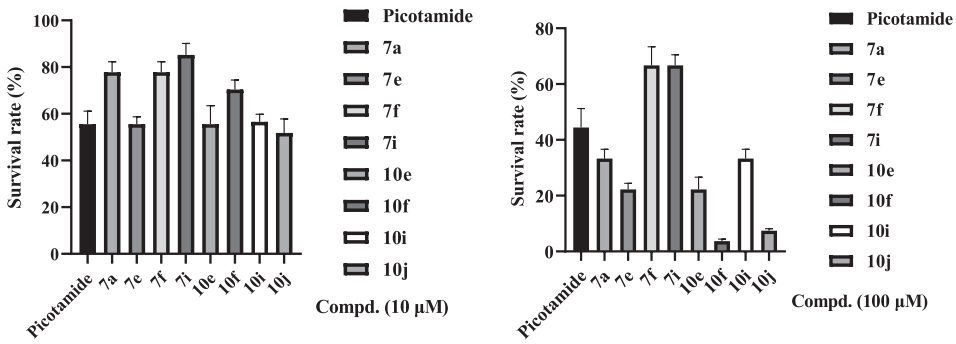

Fig. 5. Cytotoxicity in vitro effect on L929 cells.

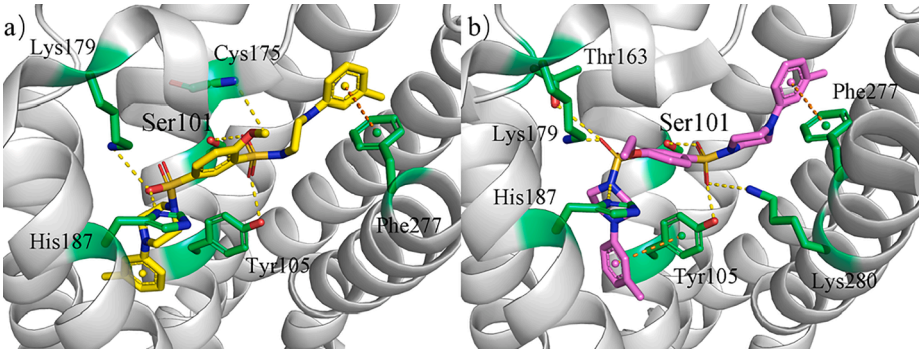

Fig. 6. a) Docking results for compound **7i**. b) Docking results for compound **10i**.

methoxy-1,3-phenylenedisulfonyl)bis(1-(*m*-tolyl)piperazine), which is the lowest cytotoxic in vitro compound among series **1** and series **2**, respectively, both of them are selected to be docked with the receptor P_2Y_{12}. The results of molecular docking show that the docking between the two compounds and P_2Y_{12} receptor is not ideal. Among them, the docking score of the compound **10i** is below one, and the docking score of the compound **7i** is even below zero. Compared with the previous design compounds with a docking score of more than 5 point, the use of piperazine groups instead of phenyl groups to introduce into the amide structural analogues of picotamide obviously does not bind to the P_2Y_{12} receptor. The carbon chain length does not change much, but the difference in aromaticity is obvious. The more precise reason that causes the decrease in the binding degree of the target compounds to the P_2Y_{12} receptor needs to be further studied and concluded.

2.3.1. *In silico prediction of molecular properties*

To predict if a chemical compound could be used orally, all newly designed compounds and previous compound **PN 113** (see Fig. 7) with outstanding anti-platelet activity are analyzed according to Lipinski's "rule of five" using Molinspiration property engine v2018.10 (www.molinspiration.com) online calculate properties.[26] Table 3 gives the results in silico prediction of molecular property.

As shown in Table 3, **PN 113** is violated the Lipinski rule of five in two places, and does not meet the requirements of the Lipinski rule of five. With the introduction of piperazine in the side chain, the MiLogP value of the newly designed target compounds is all less than 5, so that target compounds except **7g** and **10g** only one violates or fully complies with the Lipinski rule of five. The drug-likeness of the target compounds is improved, it provides new vitality for the design of new antiplatelet drugs.

Table 3
In silico prediction of molecular properties for new design compounds.

Code Rule	MW <500	MiLogP ≤5	HBA ≤10	HBD ≤5	n violation ≤1	TPSA <160 Å^2	Volume
7a	432.57	0.33	9	0	0	90.47	369.44
7b	460.62	1.08	9	0	0	90.47	403.04
7c	488.68	1.68	9	0	0	90.47	436.22
7d	556.71	3.73	9	0	1	90.47	479.14
7e	584.76	3.13	9	0	1	90.47	512.74
7f	592.69	3.96	9	0	1	90.47	489.00
7g	616.76	3.74	11	0	2	108.94	530.23
7h	584.76	4.53	9	0	1	90.47	512.26
7i	584.76	4.58	9	0	1	90.47	512.26
7j	584.76	4.62	9	0	1	90.47	512.26
10a	446.60	0.71	9	0	0	90.47	386.24
10b	474.65	1.46	9	0	0	90.47	419.85
10c	502.70	2.05	9	0	1	90.47	453.02
10d	570.74	4.10	9	0	1	90.47	495.94
10e	598.79	3.50	9	0	1	90.47	529.54
10f	606.72	4.33	9	0	1	90.47	505.80
10g	630.79	4.12	11	0	2	108.94	547.03
10h	589.79	4.90	9	0	1	90.47	529.06
10i	589.79	4.95	9	0	1	90.47	529.06
10j	589.79	5.00	9	0	1	90.47	529.06
PN 113	526.64	8.07	5	2	2	67.43	491.60

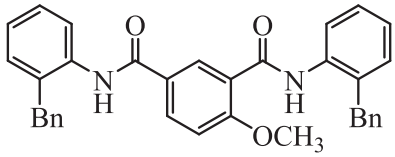

N^1, N^3-bis(2-benzylphenyl)-4-methoxyisophthalamide

PN 113: IC_{50}= 0.02 uM (ADP as an inducer)

Fig. 7. Structure of PN 113.

2.3.2. *In silico ADME prediction*

Favorable ADME has been identified as the major cause of success for

new drug molecules development.[27] Thus, with the objective of increasing the success rate of newly designed compounds reaching development, in silico ADMET prediction studies are performed using PreADMET online server (http://www.bmdrc.org). Table 4 gives the in silico ADME prediction results of eight compounds with better activities in ADP, AA or collagen test channel, and in silico molecular property prediction results of other twelve target compounds are given in Table S1.

As shown in Table 4, eight compounds express > 90% HIA values, which exhibit good permeation of across the membrane. The results of Caco-2 cell permeability in vitro indicates that all compounds exhibit moderate permeation. The MDCK cell permeability test in vitro shows the permeation of eight target compounds < 25 nm/s, indicating low permeability. The data of in vitro skin permeability shows that all newly designed compounds exhibit negative permeability values, which indicates that transdermal mode of administration is not the suitable means to administer all newly designed compounds. In addition, newly designed compounds are predicted to possess > 90% plasma protein binding (PPB) except three compounds **7a**, **7e** and **10e**, indicating decrease excretion and increase half-life.

In general, most newly designed compounds including compound **7i** and **10i** present satisfactory drug-like characteristics and ADME properties.

3. Conclusion

In order to discover antiplatelet drugs with novel structures and expand our research scope, using anisole and phenylethyl ether as starting materials, respectively, through chlorosulfonation and amination reaction, total twenty target compounds, including ten 4-methoxy-1,3-benzenedisulfonyl bis(1-hydrocarbylpiperazines) **7a-j** of series **1** and ten 4-ethoxy-1,3-benzenedisulfonyl bis(1-hydrocarbyl piperazines) **10a-j** of series **2**, are synthesized. And their chemical structure has been confirmed by ^{1}H NMR, ^{13}C NMR, IR and ESI-MS.

With aspirin and picotamide as positive control drugs, and with ADP, AA or collagen as an inducer, respectively, the Born turbidimetric method was used to screen the anti-platelet activity in vitro of all target compounds **7a-j** and **10a-j** at a concentration of 1.3 μM. It was found in this study that compound **10i**, **10j** and **7i** have the highest in vitro platelet aggregation inhibition rate in a test channel of ADP, AA or collagen in turn, respectively. And of which, the activity in vitro of five compounds **7a**, **7c**, **7i**, **10e** and **10f** for collagen was higher than both picotamide and aspirin. In the ADP and AA test channels, compounds with an inhibition rate greater than 33% were selected, and corresponding IC_{50} values were obtained by calculation. According to the results of IC_{50} value, the in vitro antiplatelet activity of one compound **10i** for ADP was higher than picotamide. And for AA, two compounds **7e** and **10j** were higher than both picotamide and aspirin, and two compounds **7h** and **10i** only higher or equivalent than aspirin. In general, compound **10i** (IC_{50}(ADP): 0.45 μM, IC_{50}(AA): 0.43 μM, Inhibition rate (collagen): 48.79%) exhibits generally stronger in vitro antiplatelet activity in the three test channels of ADP, AA and collagen.

Further, eight compounds **7a**, **7e**, **7f**, **7i**, **10e**, **10f**, **10i** and **10j** exhibiting the high activity in one or two test channels, were subjected to cytotoxicity test on L929 by CCK-8 method. And the result shows that among them, the in vitro cytotoxicity of seven compounds **7a**, **7e**, **7f**, **7i**, **10e**, **10f** and **10i** showed lower than or similar to the control drug picotamide at 10 μM, while at the higher concentration of 100 μM, merely two compounds **7f** and **7i** exhibited higher cell survival rate than that of picotamide. And compound **7i** has lowest in vitro cytotoxicity at two test concentrations.

In addition, two compounds **7i** and **10i**, as representatives of series **1** and series **2**, respectively, are selected for simulation analysis as two most likely to dock with the receptor P_2Y_{12}. In silico molecular property and ADME (absorption, distribution, metabolism and excretion) of all synthesized compounds were predicted by using Molinspiration property engine v2018.10 and PreADMET online servers, respectively.

Compared with other series of compounds obtained by introducing the phenyl group in the previous stage, the water solubility of the compound synthesized by introducing the piperazine group in this study has been improved, so that the solvent that can be used for recrystallization is increased. Compared with previous work, the compounds of two series **1** and series **2** of obtained after the introduction of piperazinyl almost have the same proportions in vitro activity higher than control drug. Most target compounds, including compound **7i** and **10i**, presented satisfactory drug-like characteristics and ADME properties. In silico prediction data of molecular properties shown that the MiLogP of newly synthesized compounds by introducing piperazine groups is indeed significantly improved. The above conclusions are limited to the scope and results of this research. More accurate conclusions might obtain after more extensive and in-depth research.

4. Experiments

4.1. Chemistry

All chemical reagents were purchased from Aladdin Industrial Corporation (China), Tianjin Heng shan (China) and Energy Chemical (China). And all chemical reagents used without further purification. The biological reagents arachidonic acid (AA) and adenosine diphosphate (ADP) were purchased from Sigma and reagents of cell viability were purchased from Beyotime Biotechnology (China). The melting points were determined with a Kofler micro melting point apparatus (uncorrected when used). Nuclear magnetic resonance (^{1}H/^{13}C NMR) spectra were recorded on a Bruker 400 MHz spectrometers (Bruker, Rheinstetten, Germany), TMS (0.05% v/v) as internal standard, pick positions are illustrated in parts per million (d) in DMSO-d_6 solution and coupling constant values (*J*) are given in Hertz. Signal multiplicities are

Table 4
In silico ADME prediction for the title compounds.

Code	Absorption				Distribution
Rule	Human intestinal absorption (%)	In vitro Caco-2 cell permeability (nm/s)	In vitro MDCK cell permeability (nm/s)	In vitro skin permeability (log K p, cm/h)	In vitro PPB (%)
	0–20 (poor)	<4 (low)	<25 (low)		>90 (strongly bound)
	20–70 (moderate)	4–70 (moderate)	25–500 (moderate)		<90 (weakly bound)
	70–100 (well)	>70 (high)	>500 (high)		
7a	99.29	21.67	0.50	−3.91	16.99
7e	97.86	21.71	0.11	−1.81	72.10
7f	97.86	21.70	0.04	−2.37	100.00
7i	97.79	21.70	0.04	−1.89	100.00
10e	97.82	21.71	0.08	−1.72	70.87
10f	97.81	21.70	0.04	−2.32	100.00
10i	97.77	21.71	0.04	−1.80	100.00
10j	97.77	21.71	0.04	−1.77	100.00
PN113	96.41	34.45	0.04	−1.72	91.93

reported by: s (singlet), d (doublet), t (triplet), q (quadruplet) and m (multiplet). Thin-layer chromatography (TLC) was performed with Merck silica gel plates and visualized with UV irradiation (254 nm). High-resolution mass spectra (HR-MS) were recorded on an Agilent 6520B UPLC-Q-TOF mass spectrometer (Agilent Technologies, Santa Clara, CA, USA). The IR spectra were taken by a PerkinElmer 843 spectrometer (KBr as diluent).

4.2. Synthesis of bis(2-chloroethyl) amine hydrochloride (2)

The corresponding (**1**) diethanolamine (5.3 g, 0.050 mol) and 25 mL dichloromethane were added into a 250 mL three-necked flask with a mechanical stirring bar, and a solution of thionyl chloride (24 g, 0.20 mol) in 20 mL dichloromethane (CH_2Cl_2) was added slowly at room temperature. After the reaction mixture was stirred at room temperature for 3 h, the solvent and excess thionyl chloride was concentrated under vacuum to obtain crude product (pale yellow solid). Then the crude product was washed with acetone to obtain white flake crystals (5.4 g), which could be used directly in the next step without further purification. Yield: 60%.

4.3. Synthesis of N-(methyl-substituted phenyl) piperazine (4h-j)

The corresponding bis(2-chloroethyl) amine hydrochloride (3.0 g, 0.017 mol) and 50 mL *n*-butanol were added into a 250 mL three-necked flask, and the reaction was allowed to raise to 130 °C. After the solid was completely dissolved, a mixture of *o*-methylaniline (1.6 g, 0.015 mol) was dissolved in 25 mL *tert*-butanol was added. This reaction mixture was refluxed at 130 °C for 24 h. After the reaction was complete, anhydrous sodium carbonate (1.6 g, 0.015 mol) was added to the reaction system in batches. After TLC (developing solvent: petroleum ether:ethyl acetate = 1:2) showed the end point of the reaction, cool overnight, and white solid precipitates out. The obtained white solid was dissolved in water (25 mL), treated with 5% sodium hydroxide solution until the pH > 12, and the aqueous layer was extracted with ethyl acetate (3 × 20 mL). Combine each of the organic phases and wash with saturated saline solution. After drying with anhydrous sodium sulfate, the reaction solution was filtered out, and concentrated under the reduced pressure to obtain brown–red oil (830 mg). Yield: 31%.

Other two intermediates **4i** and **4j**were prepared in the same manner.

4.4. Synthesis of intermediates 4-methoxybenzene-1,3-disulfonyl chloride (6)

Intermediates (**6**) 4-methoxybenzene-1,3-disulfonyl chloride was synthesized according to the literature in 2015.[20]

4.5. Synthesis of intermediates 4-ethoxybenzene-1,3-disulfonyl chloride (9)

Intermediates (**9**) 4-ethoxy-1,3-benzenedisulfonyl chloride was synthesized according to the literature method in 2019.[21]

4.6. General procedure for synthesis of target compounds (Take N^1,N^3-di (4-methoxy-1,3–phenylene-disulfonyl)bis(1-methylpiperazine) (7a) as an example)

N-methylpiperazine (600 mg 6.0 mmol) was placed in a 100 mL round bottom flask and 20 mL CH_2Cl_2 was added to dissolved it. Under ice bath condition, slowly added dropwise a mixed solution of 4-methoxy-1,3-benzenedisulfonyl chloride (1.0 g, 3.0 mmol) in 10 mL CH_2Cl_2. During the reaction, 3–4 drops of triethylamine was added as an acid binding agent. The reaction process and end point were monitored by TLC (developing solvent: petroleum ether: ethyl acetate = 1:1) at room temperature. Concentrate the reaction solution and evaporate the solvent under reduced pressure. And wash it with 10 mL 5% sodium hydroxide solution and 30 mL water, respectively to obtain the crude product. The crude product was recrystallized from ethanol to obtain white solid powder (760 mg).

4.6.1. N^1,N^3-di(4-methoxy-1,3-phenylenedisulfonyl)bis(1-methylpiperazine) (7a)

Following the general procedure, compound **7a** was synthesized from 600 mg (6.0 mmol) of *N*-methylpiperazine, 1.0 g (3.0 mmol) intermediate (**6**). It was generated as white solid powder (760 mg). Yield = 59%; m.p: 189–190 ℃ (Ethanol); IR (KBr, cm^{-1}): 2937 (CH), 2793, 2361, 1591, 1488 (C═C), 1457, 1395, 1348, 1290 (SO_2), 1168, 1146 (SO_2), 1066, 1012, 944, 733, 605, 557; ^{1}H NMR (400 MHz, $CDCl_3$) δ 8.27 (d, J = 2.3 Hz, 1H, 2-H), 7.90 (dd, J = 8.7, 2.3 Hz, 1H, 6-H), 7.11 (d, J = 8.8 Hz, 1H, 5-H), 3.99 (s, 3H, OCH_3), 3.30 (s, 4H, piperazine-H), 3.04 (s, 4H, piperazine-H), 2.48 (s, 8H, piperazine-H), 2.31 (s, 3H, N-CH_3), 2.27 (s, 3H, N-CH_3); ^{13}C NMR (101 MHz, $CDCl_3$) δ 160.1 (4-C), 134.3, 131.6, 127.9, 127.8, 112.5, 56.7 (O-CH_3), 54.8, 54.0, 46.0, 45.9 (N-CH_3), 45.8 (N-CH_3); HR ESI-MS (*m/z*): 433.1501 $[M+H]^+$ found: 433.1579.

4.6.2. N^1,N^3–di(4-methoxy-1,3-phenylenedisulfonyl)bis(1-ethylpiperazine) (7b)

Following the general procedure, compound **7b** was synthesized from 750 mg (6.0 mmol) of *N*-ethylpiperazine, 1.0 g (3.0 mmol) intermediate (**6**). It was generated as white solid powder (630 mg). Yield = 46%; m.p: 181–182 ℃ (Ethanol); IR (KBr, cm^{-1}): 2967, 2929 (CH), 2807, 2362, 1591, 1486 (C═C), 1349, 1327 (SO_2), 1289, 1260, 1168 (SO_2), 1062, 1012, 949, 845, 738, 603, 556, 524; ^{1}H NMR (400 MHz, $CDCl_3$) δ 8.28 (d, J = 2.2 Hz, 1H, 2-H), 7.90 (dd, J = 8.7, 2.2 Hz, 1H, 6-H), 7.10 (d, J = 8.7 Hz, 1H, 5-H), 3.99 (s, 3H, OCH_3), 3.31 (s, 4H, piperazine-H), 3.05 (s, 4H, piperazine-H), 2.52 (s, 8H, piperazine-H), 2.45 (m, 2H, N-$\underline{CH_2}CH_3$), 2.43–2.37 (m, 2H, N-$\underline{CH_2}CH_3$), 1.08 (t, J = 7.2 Hz, 3H, N-$CH_2\underline{CH_3}$), 1.03 (t, J = 7.2 Hz, 3H, N-$CH_2\underline{CH_3}$); ^{13}C NMR (101 MHz, $CDCl_3$) δ 160.1 (4-C), 134.3, 131.7, 127.6, 112.5, 56.7 (OCH_3), 52.5, 52.2, 52.0 (N-$\underline{CH_2}CH_3$), 51.8 (N-$\underline{CH_2}CH_3$), 46.2, 46.1, 12.0 (N-$CH_2\underline{CH_3}$), 12.0 (N-$CH_2\underline{CH_3}$); HR ESI-MS (*m/z*): 461.1908 $[M+H]^+$ found: 461.1892.

4.6.3. N^1,N^3–di(4-methoxy-1,3-phenylenedisulfonyl)bis(1-isopropylpiperazine) (7c)

Following the general procedure, compound **7c** was synthesized from 840 mg (6.0 mmol) of *N*-isopropylpiperazine, 1.0 g (3.0 mmol) intermediate (**6**). It was generated as white solid powder (410 mg). Yield = 26%; m.p: 166–167 ℃ (Benzene-Petroleum Ether); IR (KBr, cm^{-1}): 2965 (CH), 2814, 1591, 1485 (C═C), 1350 (SO_2), 1288, 1162 (SO_2), 1063, 1011, 974, 943, 739, 604, 554; ^{1}H NMR (400 MHz, $CDCl_3$) δ 8.27 (d, J = 2.0 Hz, 1H, 2-H), 7.90 (dd, J = 8.7, 2.0 Hz, 1H, 6-H), 7.10 (d, J = 8.7 Hz, 1H, 5-H), 4.00 (s, 3H, OCH_3), 3.31 (s, 4H, piperazine-H), 3.03 (s, 4H, piperazine-H), 2.74–2.65 (m, 2H, *N*-$\underline{CH}(CH_3)_2$), 2.63 (s, 8H, piperazine-H), 1.05 (d, J = 5.9 Hz, 6H, *N*-$CH(\underline{CH_3)_2}$), 1.00 (d, J = 6.5 Hz, 6H, *N*-$CH(\underline{CH_3)_2}$); ^{13}C NMR (101 MHz, $CDCl_3$) δ 160.2 (4-C), 134.2, 131.7, 128.4, 127.7, 112.6, 56.7 (OCH_3), 54.7 (*N*-$\underline{CH}(CH_3)_2$), 54.4 (*N*-$\underline{CH}(CH_3)_2$), 48.5, 47.8, 46.5, 46.4, 18.4 (2 × *N*-$CH(\underline{CH_3)_2}$); HR ESI-MS (*m/z*): 489.2127 $[M+H]^+$ found: 489.2238.

4.6.4. N^1,N^3–di(4-methoxy-1,3-phenylenedisulfonyl)bis(1-phenylpiperazine) (7d)

Following the general procedure, compound **7d** was synthesized from 530 mg (3.3 mmol) of *N*-Phenylpiperazine, 500 mg (1.6 mmol) intermediate (**6**). It was generated as white solid powder (490 mg). Yield = 55%; m.p: 297–298 ℃ (*N*, *N*-Dimethylformamide-Water); IR (KBr, cm^{-1}): 2924, 2854 (CH), 2362, 2336, 1594, 1489 (C═C), 1455, 1393, 1342 (SO_2), 1288, 1235, 1161, (SO_2), 948, 740, 556; ^{1}H NMR (400 MHz, DMSO) δ 8.04 (d, J = 9.0 Hz, 2H, Ar-H), 7.52 (d, J = 9.1 Hz, 1H, Ar-H), 7.19 (t, J = 7.3 Hz, 4H, Ar-H), 6.90 (d, J = 7.0 Hz, 4H, Ar-H), 6.79 (t, J = 6.8 Hz, 2H, Ar-H), 4.02 (s, 3H, OCH_3), 3.29 (s, 4H,

piperazine-H), 3.21 (s, 4H, piperazine-H), 3.15 (s, 4H, piperazine-H), 3.04 (s, 4H, piperazine-H); ^{13}C NMR (101 MHz, $CDCl_3$) δ 159.6 (4-C), 150.5, 134.2, 131.6, 129.2, 129.2, 127.7, 127.3, 120.9, 116.9, 116.9, 113.4, 65.7 (OCH_3), 49.8, 49.0, 46.0, 14.5; HR ESI-MS (*m/z*): 557.1892 $[M+H]^+$ found: 557.1893.

4.6.5. N^1,N^3–di(4-methoxy-1,3-phenylenedisulfonyl)bis(1-benzylpiperazine) (7e)

Following the general procedure, compound **7e** was synthesized from 580 mg (3.3 mmol) of *N*-benzylpiperazine, 500 mg (1.6 mmol) intermediate (**6**). It was generated as white solid powder (540 mg). Yield = 58%; m.p: 210–212 ℃ (Acetone); IR (KBr, cm^{-1}): 2923 (CH), 2361, 1646, 1588 (C═C), 1458, 1396, 1357 (SO_2), 1286, 1165 (SO_2), 1069, 941, 848, 735, 698, 600, 554; ^{1}H NMR (400 MHz, $CDCl_3$) δ 8.26 (d, J = 2.2 Hz, 1H, 2-H), 7.90 (dd, J = 8.7, 2.2 Hz, 1H, 6-H), 7.28 (m, 10*H*, Ar-H), 7.11 (d, J = 8.7 Hz, 1H, 5-H), 4.00 (s, 3H, OCH_3), 3.54 (s, 2H, N-CH_2-), 3.49 (s, 2H, N-CH_2-), 3.31 (s, 4H, piperazine-H), 3.03 (s, 4H, piperazine-H), 2.53 (s, 8H, piperazine-H); ^{13}C NMR (101 MHz, $CDCl_3$) δ 160.1 (4-C), 137.5, 137.4, 134.3, 131.6, 129.3, 129.2, 128.5, 128.5, 127.9, 127.8, 127.5, 112.6, 62.8 (N-CH_2-), 62.6 (N-CH_2-), 56.7 (OCH_3), 52.8, 52.1, 46.2, 46.1; HR ESI-MS (*m/z*): 585.2201 $[M+H]^+$ found: 585.2205.

4.6.6. N^1,N^3–di(4-methoxy-1,3-phenylenedisulfonyl)bis(1-(2-fluorophenyl)piperazine) (7f)

Following the general procedure, compound **7f** was synthesized from 590 mg (3.3 mmol) of *N*-(2-fluorophenyl)piperazine, 500 mg (1.6 mmol) intermediate (**6**). It was generated as white solid powder (620 mg). Yield = 65%; m.p: 237–238 ℃ (Acetone); IR (KBr, cm^{-1}): 3415, 3134 (=CH), 1591, 1502 (C═C), 1484, 1397, 1351 (SO_2), 1335, 1289, 1239, 1158 (SO_2), 948, 744, 556; ^{1}H NMR (400 MHz, $CDCl_3$) δ 8.36 (d, J = 2.2 Hz, 1H, 2-H), 7.98 (dd, J = 8.7, 2.3 Hz, 1H, 6-H), 7.18 (d, J = 8.8 Hz, 1H, 5-H), 7.11–7.03 (m, 3H, Ar-H), 6.98 (m, 5H, Ar-H), 4.06 (s, 3H, OCH_3), 3.53–3.44 (m, 4H, piperazine-H), 3.21 (d, J = 4.6 Hz, 4H, piperazine-H), 3.16 (dd, J = 10.3, 6.1 Hz, 8H, piperazine-H); ^{13}C NMR (101 MHz, $CDCl_3$) δ 160.2 (4-C), 157.0 (1-C), 154.6 (3-C), 139.2, 134.4, 131.8, 127.9, 127.9, 124.8, 124.8, 124.7, 123.6, 123.6, 119.6, 119.5, 116.5, 116.3, 112.8, 100.1, 56.8 (OCH_3), 50.8, 50.0, 46.4, 46.3; HR ESI-MS (*m/z*): 593.1700 $[M+H]^+$ found: 593.1704.

4.6.7. N^1,N^3–di(4-methoxy-1,3-phenylenedisulfonyl)bis(1-(2-methoxyphenyl)piperazine) (7g)

Following the general procedure, compound **7g** was synthesized from 880 mg (4.6 mmol) of *N*-(2-methoxyphenyl)piperazine, 700 mg (2.3 mmol) intermediate (**6**). It was generated as white solid powder (680 mg). Yield = 48%; m.p: 208–209 ℃ (Acetone); IR (KBr, cm^{-1}): 3129 (=CH), 2837 (CH), 1589, 1501 (C═C), 1395 (SO_2), 1242, 1165 (SO_2), 1067, 1023, 948, 844, 744, 554; ^{1}H NMR (400 MHz, $CDCl_3$) δ 8.36 (d, J = 2.1 Hz, 1H, 2-H), 7.96 (dd, J = 8.7, 2.1 Hz, 1H, 6-H), 7.16 (d, J = 8.8 Hz, 1H, 5-H), 7.08–7.00 (m, 2H, Ar-H), 6.93 (dd, J = 6.6, 3.6 Hz, 4H, Ar-H), 6.86 (t, J = 8.2 Hz, 2H, Ar-H), 4.04 (s, 3H, OCH_3), 3.85 (s, 3H, Ph-$\underline{OCH_3}$), 3.82 (s, 3H, Ph-$\underline{OCH_3}$), 3.48 (s, 4H, piperazine-H), 3.22 (s, 4H, piperazine-H), 3.13 (s, 8H, piperazine-H); ^{13}C NMR (101 MHz, $CDCl_3$) δ 160.3 (4-C), 152.2, 140.5, 140.3, 134.4, 132.0, 127.8, 127.7, 123.9, 121.2, 121.1, 118.7, 118.6, 112.7, 111.3, 56.8 (OCH_3), 55.5 (2 × Ph-$\underline{OCH_3}$), 50.8, 50.0, 46.5, 46.4; HR ESI-MS (*m/z*): 617.2104 $[M+H]^+$ found: 617.2104.

4.6.8. N^1,N^3–di(4-methoxy-1,3-phenylenedisulfonyl)bis(1-(o-tolyl)piperazine) (7h)

Following the general procedure, compound **7h** was synthesized from 550 mg (3.1 mmol) of *N*-(2-methylphenyl)piperazine, 470 mg (1.6 mmol) intermediate (**6**). It was generated as white solid powder (230 mg). Yield = 26%; m.p: 227–229 ℃ (*N*, *N*-Dimethylformamide-Water); IR (KBr, cm^{-1}): 3446, 2950, 2850 (CH), 1592 (C═C), 1489, 1448, 1347 (SO_2), 1285, 1260, 1226, 1162 (SO_2), 1067, 1012, 951, 845, 767, 735, 600, 554; ^{1}H NMR (400 MHz, $CDCl_3$) δ 8.37 (d, J = 1.9 Hz, 1H, 2-H), 8.00 (dd, J = 8.7, 1.9 Hz, 1H, 6-H), 7.25 (d, J = 8.8 Hz, 1H, 5-H), 7.21–7.15 (m, 4H, Ar-H), 7.02 (dd, J = 9.8, 7.7 Hz, 4H, Ar-H), 4.09 (s, 3H, OCH_3), 3.46 (s, 4H, piperazine-H), 3.19 (s, 4H, piperazine-H), 3.04–2.92 (m, 8H, piperazine-H), 2.27 (s, 3H, Ph-$\underline{CH_3}$), 2.21 (s, 3H, Ph-$\underline{CH_3}$); ^{13}C NMR (101 MHz, $CDCl_3$) δ 160.2 (4-C), 150.8 (1-C), 150.6 (3-C), 134.3, 132.8, 132.7, 131.6, 131.3, 128.2, 128.1, 126.9, 126.8, 124.1, 119.5, 119.4, 112.8, 56.8 (OCH_3), 51.9, 51.2, 46.8, 46.6, 17.9 (2 × Ph-$\underline{CH_3}$); HR ESI-MS (*m/z*): 585.2196 $[M+H]^+$ found: 585.2205.

4.6.9. N^1,N^3–di(4-methoxy-1,3-phenylenedisulfonyl)bis(1-(m-tolyl)piperazine) (7i)

Following the general procedure, compound **7i** was synthesized from 600 mg (3.4 mmol) of *N*-(3-methylphenyl)piperazine, 510 mg (1.7 mmol) intermediate (**6**). It was generated as white solid powder (500 mg). Yield = 50%; m.p: 284–285 ℃ (*N*, *N*-Dimethylformamide-Water); IR (KBr, cm^{-1}): 2827 (CH), 2362, 1593 (C═C), 1489, 1451, 1391, 1343 (SO_2), 1250, 1161 (SO_2), 1065, 1007, 954, 848, 778, 741, 694, 556; ^{1}H NMR (400 MHz, DMSO) δ 8.04 (d, J = 8.8 Hz, 2H, Ar-H), 7.52 (d, J = 8.5 Hz, 1H, Ar-H), 7.07 (t, J = 7.8 Hz, 2H, Ar-H), 6.75–6.66 (m, 4H, Ar-H), 6.62 (d, J = 6.7 Hz, 2H, Ar-H), 4.02 (s, 3H, OCH_3), 3.28 (s, 4H, piperazine-H), 3.19 (s, 4H, piperazine-H), 3.12 (s, 4H, piperazine-H), 3.03 (s, 4H, piperazine-H), 2.21 (s, 6H, Ph-$\underline{CH_3}$); ^{13}C NMR (101 MHz, DMSO) δ 160.5 (4-C), 150.7, 138.5, 130.6, 129.2, 126.7, 120.9, 117.2, 115.0, 113.7, 57.4 (OCH_3), 49.0, 48.3, 46.2, 46.0, 21.7 (2 × Ph-$\underline{CH_3}$); HR ESI-MS (*m/z*): 585.2198 $[M+H]^+$ found: 585.2205.

4.6.10. N^1,N^3–di(4-methoxy-1,3-phenylenedisulfonyl)bis(1-(p-tolyl)piperazine) (7j)

Following the general procedure, compound **7j** was synthesized from 1.6 g (9.3 mmol) of *N*-(4-methylphenyl)piperazine, 1.4 g (4.7 mmol) intermediate (**6**). It was generated as white solid powder (990 mg). Yield = 36%; m.p: 300–302 ℃ (*N*, *N*-Dimethylformamide-Water); IR (KBr, cm^{-1}): 3446, 2362, 1591, 1516 (C═C), 1484, 1392, 1343 (SO_2), 1290, 1237, 1162 (SO_2), 948, 741, 601, 541; ^{1}H NMR (400 MHz, DMSO) δ 8.04 (d, J = 8.1 Hz, 2H, Ar-H), 7.52 (d, J = 8.3 Hz, 1H, Ar-H), 7.00 (d, J = 8.0 Hz, 4H, Ar-H), 6.80 (d, J = 8.3 Hz, 4H, Ar-H), 4.02 (s, 3H, OCH_3), 3.27 (s, 4H, piperazine-H), 3.14 (s, 4H, piperazine-H), 3.07 (s, 4H, piperazine-H), 3.03 (s, 4H, piperazine-H), 2.17 (s, 3H, Ph-$\underline{CH_3}$), 2.16 (s, 3H, Ph-$\underline{CH_3}$); ^{13}C NMR (101 MHz, $CDCl_3$) δ 160.0 (4-C), 150.6 (1-C), 150.4 (3-C), 134.2, 132.6, 132.6, 131.4, 131.1, 128.0, 127.9, 126.7, 126.7, 124.0, 123.9, 119.3, 119.3, 112.7, 56.6 (OCH_3), 51.8, 51.0, 46.6, 46.5, 17.7 (2 × Ph-$\underline{CH_3}$); HR ESI-MS (*m/z*): 585.2211 $[M+H]^+$ found: 585.2205.

4.6.11. N^1,N^3–di(4-ethoxy-1,3-phenylenedisulfonyl)bis(1-methylpiperazine) (10a)

Following the general procedure, compound **10a** was synthesized from 5.4 g (5.4 mmol) of *N*-methylpiperazine, 860 mg (2.7 mmol) intermediate (**9**). It was generated as white solid powder (570 mg). Yield = 48%; m.p: 147–148 ℃ (Petroleum ether-Ethyl aceta); IR (KBr, cm^{-1}): 2982, 2939 (CH), 2850, 2798, 1588 (C═C), 1456, 1394, 1356, 1333, 1290 (SO_2), 1172 (SO_2), 1068, 943, 842, 787, 746, 603, 567, 520; ^{1}H NMR (400 MHz, $CDCl_3$) δ 8.26 (d, J = 2.3 Hz, 1H, 2-H), 7.86 (dd, J = 8.7, 2.3 Hz, 1H, 6-H), 7.08 (d, J = 8.8 Hz, 1H, 5-H), 4.22 (q, J = 7.0 Hz, 2H, O$\underline{CH_2}$$CH_3$), 3.31 (s, 4H, piperazine-H), 3.03 (s, 4H, piperazine-H), 2.47 (d, J = 4.6 Hz, 4H, piperazine-H), 2.45 (d, J = 4.7 Hz, 4H, piperazine-H), 2.30 (s, 3H, N-CH_3), 2.26 (s, 3H, N-CH_3), 1.52 (t, J = 7.0 Hz, 3H, $OCH_2\underline{CH_3}$); ^{13}C NMR (101 MHz, $CDCl_3$) δ 159.6 (4-C), 134.2, 131.7, 127.8, 127.4, 113.3, 65.8 (O$\underline{CH_2}$$CH_3$), 54.8 (N-$CH_3$), 54.0 (N-$CH_3$), 46.1, 46.0, 46.0, 45.8, 14.6 ($OCH_2\underline{CH_3}$); HR ESI-MS (*m/z*): 447.1758 $[M+H]^+$ found: 447.1736.

4.6.12. N^1,N^3–di(4-ethoxy-1,3-phenylenedisulfonyl)bis(1-ethylpiperazine) (10b)

Following the general procedure, compound **10b** was synthesized

from 360 mg (3.1 mmol) of *N*-ethylpiperazine, 500 mg (1.6 mmol) intermediate (**9**). It was generated as white solid powder (260 mg). Yield = 35%; m.p: 170–171 ℃ (Ethanol); IR (KBr, cm^{-1}): 3131 (=CH), 2811 (CH), 1587 (C═C), 1401 (SO_2), 1350, 1283, 1176, 1150 (SO_2), 1107, 1062, 1032, 960, 840, 743, 598, 569, 520; ^{1}H NMR (400 MHz, $CDCl_3$) δ 8.24 (d, J = 3.6 Hz, 1H, 2-H), 7.85 (dd, J = 9.2, 7.0 Hz, 1H, 6-H), 7.07 (d, J = 8.7 Hz, 1H, 5-H), 4.19 (dd, J = 14.4, 7.5 Hz, 2H, O$\underline{CH_2}CH_3$), 3.30 (s, 4H, piperazine-H), 3.02 (s, 4H, piperazine-H), 2.49 (s, 8H, piperazine-H), 2.40 (dt, J = 14.1, 7.3 Hz, 4H, N-$\underline{CH_2}CH_3$), 1.56–1.46 (m, 3H, $OCH_2\underline{CH_3}$), 1.10–0.95 (m, 6H, N-$CH_2\underline{CH_3}$); ^{13}C NMR (101 MHz, $CDCl_3$) δ 159.7 (4-C), 134.2, 131.8, 127.7, 127.3, 113.3, 65.7 (O$\underline{CH_2}CH_3$), 52.6, 52.2, 51.9, 51.8, 46.2 (2 × N-$\underline{CH_2}CH_3$), 14.6 (O-$CH_2\underline{CH_3}$), 12.0 (N-$CH_2\underline{CH_3}$); HR ESI-MS (*m/z*): 475.2068 $[M+H]^+$ found: 475.2049.

4.6.13. N^1,N^3–di(4-ethoxy-1,3-phenylenedisulfonyl)bis(1-isopropylpiperazine) (10c)

Following the general procedure, compound **10c** was synthesized from 770 mg (6.0 mmol) of *N*-isopropylpiperazine, 1.0 g (3.0 mmol) intermediate (**9**). It was generated as white solid powder (1.2 g). Yield = 77%; m.p: 175–176 ℃ (Ethanol); IR (KBr, cm^{-1}): 3416, 3132 (=CH), 2968 (CH), 1588 (C═C), 1470, 1397 (SO_2), 1348, 1288, 1175 (SO_2), 1174, 952, 743, 601, 568; ^{1}H NMR (400 MHz, $CDCl_3$) δ 8.27 (d, J = 2.0 Hz, 1H, 2-H), 7.86 (dd, J = 8.7, 2.0 Hz, 1H, 6-H), 7.07 (d, J = 8.7 Hz, 1H, 5-H), 4.22 (q, J = 6.9 Hz, 2H, O$\underline{CH_2}CH_3$), 3.30 (s, 4H, piperazine-H), 3.02 (s, 4H, piperazine-H), 2.72–2.64 (m, 2H, *N*-CH($\underline{CH_3}$)$_2$), 2.59 (s, 8H, piperazine-H), 1.53 (t, J = 6.9 Hz, 3H, $OCH_2\underline{CH_3}$), 1.04 (d, J = 6.4 Hz, 6H, *N*-CH($\underline{CH_3}$)$_2$), 1.00 (d, J = 6.5 Hz, 6H, *N*-CH($\underline{CH_3}$)$_2$); ^{13}C NMR (101 MHz, $CDCl_3$) δ 159.7 (4-C), 134.1, 131.8, 127.7, 127.4, 113.3, 65.7 (O$\underline{CH_2}CH_3$), 54.6 (*N*-$\underline{CH}(CH_3)_2$), 54.4 (*N*-$\underline{CH}(CH_3)_2$), 48.5, 47.8, 46.5, 18.4 (*N*-CH($\underline{CH_3}$)$_2$), 14.6 ($OCH_2\underline{CH_3}$); HR ESI-MS (*m/z*): 503.2383 $[M+H]^+$ found: 503.2362.

4.6.14. N^1,N^3–di(4-ethoxy-1,3-phenylenedisulfonyl)bis(1-phenylpiperazine) (10d)

Following the general procedure, compound **10d** was synthesized from 1.0 g (6.3 mmol) of *N*-phenylpiperazine, 1.0 g (3.0 mmol) intermediate (**9**). It was generated as white solid powder (660 mg). Yield = 37%; m.p: 297–298 ℃ (N, *N*-Dimethylformamide-Water); IR (KBr, cm^{-1}): 3131 (=CH), 1595 (C═C), 1401 (SO_2), 1234, 1159 (SO_2), 952, 739, 602, 555; ^{1}H NMR (400 MHz, $CDCl_3$) δ 8.36 (d, J = 2.3 Hz, 1H, 2-H), 7.94 (dd, J = 8.7, 2.3 Hz, 1H, 6-H), 7.28 (dt, J = 7.2, 5.6 Hz, 4H, Ar-H), 7.14 (d, J = 8.8 Hz, 1H, 5-H), 6.91 (m, 6H, Ar-H), 4.27 (q, J = 7.0 Hz, 2H, O$\underline{CH_2}CH_3$), 3.47 (s, 4H, piperazine-H), 3.25 (dd, J = 11.8, 6.7 Hz, 8H, piperazine-H), 3.20–3.12 (m, 4H, piperazine-H), 1.56 (t, J = 7.0 Hz, 3H, $OCH_2\underline{CH_3}$); ^{13}C NMR (101 MHz, $CDCl_3$) δ 159.8 (4-C), 150.8 (1-C), 150.6 (3-C), 134.4, 131.7, 129.4, 127.8, 127.5, 121.0, 117.1, 117.1, 113.5, 65.9 (O$\underline{CH_2}CH_3$), 50.0, 49.2, 46.2, 46.1, 14.6 ($OCH_2\underline{CH_3}$); HR ESI-MS (*m/z*): 571.2039 $[M+H]^+$ found: 571.2049.

4.6.15. N^1,N^3–di(4-ethoxy-1,3-phenylenedisulfonyl)bis(1-benzylpiperazine) (10e)

Following the general procedure, compound **10e** was synthesized from 660 mg (3.8 mmol) of *N*-benzylpiperazine, 600 mg (1.9 mmol) intermediate (**9**). It was generated as white solid powder (510 mg). Yield = 45%; m.p: 194–195 ℃ (Methanol); IR (KBr, cm^{-1}): 3411, 3132 (=CH), 1619, 1401 (SO_2), 1166 (SO_2), 742, 619, 567, 477; ^{1}H NMR (400 MHz, $CDCl_3$) δ 8.26 (d, J = 2.1 Hz, 1H, 2-H), 7.86 (dd, J = 8.7, 2.1 Hz, 1H, 6-H), 7.32 (dd, J = 9.9, 6.3 Hz, 6H, Ar-H), 7.24 (d, J = 7.2 Hz, 4H, Ar-H), 7.08 (d, J = 8.7 Hz, 1H, 5-H), 4.23 (q, J = 6.9 Hz, 2H, O$\underline{CH_2}CH_3$), 3.53 (s, 2H, N-$\underline{CH_2}$-Ph), 3.49 (s, 2H, N-$\underline{CH_2}$-Ph), 3.32 (s, 4H, piperazine-H), 3.02 (s, 4H, piperazine-H), 2.52 (s, 8H, piperazine-H), 1.52 (t, J = 7.0 Hz, 3H, $OCH_2\underline{CH_3}$); ^{13}C NMR (101 MHz, $CDCl_3$) δ 159.7 (4-C), 137.6, 134.2, 131.7, 129.3, 129.1, 128.5, 128.5, 127.9, 127.5, 127.4, 113.3, 65.8 (O$\underline{CH_2}CH_3$), 62.9 (N-$\underline{CH_2}$-Ph), 62.6 (N-$\underline{CH_2}$-Ph), 52.9, 52.1, 46.3, 14.6 ($OCH_2\underline{CH_3}$); HR ESI-MS (*m/z*): 599.2385 $[M+H]^+$ found: 599.2362.

4.6.16. N^1,N^3–di(4-ethoxy-1,3-phenylenedisulfonyl)bis(1-(2-fluorophenyl)piperazine) (10f)

Following the general procedure, compound **10f** was synthesized from 560 mg (3.1 mmol) of *N*-(2-fluorophenyl)piperazine, 500 mg (1.6 mmol) intermediate (**9**). It was generated as white solid powder (420 mg). Yield = 44%; m.p: 178–179 ℃ (Ethanol); IR (KBr, cm^{-1}): 3132 (=CH), 1616, 1589 (C═C), 1499, 1401 (SO_2), 1287, 1239, 1164 (SO_2), 949, 732, 600, 571; ^{1}H NMR (400 MHz, $CDCl_3$) δ 8.36 (d, J = 2.3 Hz, 1H, 2-H), 7.94 (dd, J = 8.7, 2.4 Hz, 1H, 6-H), 7.15 (d, J = 8.8 Hz, 1H, 5-H), 7.09 (dd, J = 7.2, 2.1 Hz, 1H), 7.07 (d, J = 2.0 Hz, 1H), 7.06–7.04 (m, 1H), 7.03–7.01 (m, 1H), 6.99 (dd, J = 5.0, 1.8 Hz, 2H), 6.97 (dd, J = 2.9, 1.5 Hz, 1H), 6.95–6.91 (m, 1H), 4.29 (q, J = 7.0 Hz, 2H, O$\underline{CH_2}CH_3$), 3.56–3.44 (m, 4H, piperazine-H), 3.21 (d, J = 4.7 Hz, 4H, piperazine-H), 3.16 (dd, J = 10.2, 5.9 Hz, 8H, piperazine-H), 1.57 (t, J = 7.0 Hz, 3H, OCH_2CH_3); ^{13}C NMR (101 MHz, $CDCl_3$) δ 159.8 (4-C), 157.0 (1-C), 154.6 (3-C), 139.3, 134.3, 131.8, 127.9, 127.5, 124.8, 124.7, 124.7, 123.6, 119.6, 119.4, 116.5, 116.3, 113.6, 65.9 (O$\underline{CH_2}CH_3$), 50.8, 50.0, 46.4, 14.7 ($OCH_2\underline{CH_3}$); HR ESI-MS (*m/z*): 607.1873 $[M+H]^+$ found: 607.1860.

4.6.17. N^1,N^3–di(4-ethoxy-1,3-phenylenedisulfonyl)bis(1-(2-methoxyphenyl)piperazine) (10g)

Following the general procedure, compound **10g** was synthesized from 840 mg (4.4 mmol) of *N*-(2-methoxyphenyl)piperazine, 700 mg (2.2 mmol) intermediate (**9**). It was generated as white solid powder (550 mg). Yield = 40%; m.p: 208–209 ℃ (Acetone); IR (KBr, cm^{-1}): 3131 (=CH), 1619, 1590 (C═C), 1499, 1401 (SO_2), 1294, 1243, 1164 (SO_2), 949, 747, 575; ^{1}H NMR (400 MHz, $CDCl_3$) δ 8.36 (d, J = 1.7 Hz, 1H, 2-H), 7.93 (dd, J = 8.6, 1.7 Hz, 1H, 6-H), 7.12 (d, J = 8.7 Hz, 1H, 5-H), 7.08–6.98 (m, 2H), 6.92 (d, J = 4.8 Hz, 4H), 6.86 (t, J = 8.0 Hz, 2H), 4.26 (q, J = 6.7 Hz, 2H, O$\underline{CH_2}CH_3$), 3.85 (s, 3H, Ph-O$\underline{CH_3}$), 3.82 (s, 3H, Ph-O$\underline{CH_3}$), 3.50 (s, 4H, piperazine-H), 3.22 (s, 4H, piperazine-H), 3.13 (s, 8H, piperazine-H), 1.56 (t, J = 6.9 Hz, 3H, $OCH_2\underline{CH_3}$); ^{13}C NMR (101 MHz, $CDCl_3$) δ 159.9 (4-C), 152.3, 140.6, 140.4, 134.3, 132.0, 127.9, 127.5, 123.8, 121.2, 118.7, 118.6, 113.5, 111.4, 65.9 (O$\underline{CH_2}CH_3$), 55.5 (2 × Ph-O$\underline{CH_3}$), 50.8, 50.1, 46.6, 46.5, 14.6 ($OCH_2\underline{CH_3}$); HR ESI-MS (*m/z*): 631.2279 $[M+H]^+$ found: 631.2260.

4.6.18. N^1,N^3–di(4-ethoxy-1,3-phenylenedisulfonyl)bis(1-(o-tolyl) piperazine) (10h)

Following the general procedure, compound **10h** was synthesized from 580 mg (3.30 mmol) of *N*-(2-methylphenyl)piperazine, 500 mg (1.6 mmol) intermediate (**9**). It was generated as white solid powder (360 mg). Yield = 37%; m.p: 174–176 ℃ (Ethanol); IR (KBr, cm^{-1}): 3131 (=CH), 1590, 1491 (C═C), 1401, 1352 (SO_2), 1293, 1260, 1225, 1166 (SO_2), 948, 757, 575; ^{1}H NMR (400 MHz, $CDCl_3$) δ 8.37 (d, J = 2.1 Hz, 1H, 2-H), 7.97 (dd, J = 8.7, 2.1 Hz, 1H, 6-H), 7.22–7.14 (m, 5H), 7.02 (dd, J = 9.0, 7.6 Hz, 4H), 4.32 (q, J = 6.9 Hz, 2H, O$\underline{CH_2}CH_3$), 3.49 (s, 4H, piperazine-H), 3.18 (s, 4H, piperazine-H), 3.05–2.93 (m, 8H, piperazine-H), 2.28 (s, 3H, Ph-$\underline{CH_3}$), 2.21 (s, 3H, Ph-$\underline{CH_3}$), 1.58 (t, J = 6.9 Hz, 3H, $OCH_2\underline{CH_3}$); ^{13}C NMR (101 MHz, $CDCl_3$) δ 159.7 (4-C), 150.8 (1-C), 150.6 (3-C), 134.3, 132.8, 132.7, 131.7, 131.3, 128.2, 127.9, 126.9, 126.8, 124.1, 124.1, 119.5, 113.5, 65.8 (O$\underline{CH_2}CH_3$), 52.0, 51.2, 46.8, 46.7, 17.9 (2 × Ph-$\underline{CH_3}$), 14.7 ($OCH_2\underline{CH_3}$); HR ESI-MS (*m/z*): 599.2369 $[M+H]^+$ found: 599.2362.

4.6.19. N^1,N^3–di(4-ethoxy-1,3-phenylenedisulfonyl)bis(1-(m-tolyl) piperazine) (10i)

Following the general procedure, compound **10i** was synthesized from 550 mg (3.1 mmol) of *N*-(3-methylphenyl)piperazine, 500 mg (1.6 mmol) intermediate (**9**). It was generated as white solid powder (440 mg). Yield = 46%; m.p: 219–220 ℃ (N, *N*-Dimethylformamide-Water); IR (KBr, cm^{-1}): 2922, 2848 (CH), 1591 (C═C), 1453, 1391, 1343 (SO_2), 1247, 1158 (SO_2), 1022, 954, 837, 779, 739, 554; ^{1}H NMR (400 MHz, DMSO) δ 8.06 (d, J = 1.5 Hz, 1H, 2-H), 8.01 (dd, J = 8.7, 1.5 Hz, 1H, 6-H), 7.50 (d, J = 8.8 Hz, 1H, 5-H), 7.07 (t, J = 7.7 Hz, 2H), 6.74–6.67 (m,

4H), 6.61 (d, $J = 7.1$ Hz, 2H), 4.31 (q, $J = 6.9$ Hz, 2H, O$\underline{CH_2}CH_3$), 3.29 (s, 4H, piperazine-H), 3.19 (s, 4H, piperazine-H), 3.13 (s, 4H, piperazine-H), 3.02 (s, 4H, piperazine-H), 2.21 (s, 6H, 2 × Ph-$\underline{CH_3}$), 1.41 (t, $J = 6.8$ Hz, 3H, $OCH_2\underline{CH_3}$); ^{13}C NMR (101 MHz, DMSO) δ 160.0 (4-C), 151.0 (1-C), 150.8 (3-C), 138.6, 135.0, 130.8, 129.3, 126.6, 126.3, 121.0, 117.2, 117.2, 115.6, 113.8, 113.8, 66.1 (O$\underline{CH_2}CH_3$), 49.0, 48.3, 46.3, 46.2, 21.8 (2 × Ph-$\underline{CH_3}$), 14.7 ($OCH_2\underline{CH_3}$); HR ESI-MS (*m/z*): 599.2379 $[M+H]^+$ found: 599.2362.

*4.6.20. N^1,N^3–di(4-ethoxy-1,3-phenylenedisulfonyl)bis(1-(p-tolyl) piperazine) (**10j**)*

Following the general procedure, compound **10j** was synthesized from 880 mg (5.0 mmol) of *N*-(4-methylphenyl)piperazine, 800 mg (2.5 mmol) intermediate (**9**). It was generated as white solid powder (400 mg). Yield = 27%; m.p: 225–226 ℃ (Acetone); IR (KBr, cm^{-1}): 2985, 2919, 2823 (CH), 1589, 1515 (C═C), 1475, 1453, 1392, 1347 (SO_2), 1236. 1160 (SO_2), 1061, 952, 814, 737, 601, 549; ^{1}H NMR (400 MHz, DMSO) δ 8.05 (d, $J = 1.5$ Hz, 1H, 2-H), 8.00 (dd, $J = 9.0$, 1.5 Hz, 1H, 6-H), 7.49 (d, $J = 8.8$ Hz, 1H, 5-H), 7.00 (d, $J = 8.2$ Hz, 4H), 6.80 (d, $J = 7.7$ Hz, 4H), 4.31 (q, $J = 6.9$ Hz, 2H, O$\underline{CH_2}CH_3$), 3.29 (s, 4H, piperazine-H), 3.14 (s, 4H, piperazine-H), 3.08 (s, 4H, piperazine-H), 3.02 (s, 4H, piperazine-H), 2.17 (s, 3H, Ph-$\underline{CH_3}$), 2.16 (s, 3H, Ph-$\underline{CH_3}$), 1.41 (t, $J = 6.9$ Hz, 3H, $OCH_2\underline{CH_3}$); ^{13}C NMR (101 MHz, DMSO) δ 159.9 (4-C), 148.7 (1-C), 148.5 (3-C), 134.9, 130.8, 129.8, 129.1, 126.7, 126.4, 116.8, 116.8, 115.5, 66.0 (O$\underline{CH_2}CH_3$), 49.5, 48.7, 46.2, 46.1, 20.4 (2 × Ph-$\underline{CH_3}$), 14.6 ($OCH_2\underline{CH_3}$); HR ESI-MS (*m/z*): 599.2353 $[M+H]^+$ found: 599.2362.

Declaration of Competing Interest

The authors declare that they have no known competing financial interests or personal relationships that could have appeared to influence the work reported in this paper.

Acknowledgments

The authors are grateful to the National Science Foundation of China (11341014), the Committee of Science and Technology of Tianjin (15JCZDJC33100) and Shenyang Pharmaceutical University of China for running platelet aggregation assays.

Appendix A. Supplementary material

Supplementary data to this article can be found online at https://doi.org/10.1016/j.bmc.2021.116390.

References

1 Chen P, Ren S, Song H, et al. Synthesis and biological evaluation of BMS-986120 and its deuterated derivatives as PAR4 antagonists. *Bioorg Med Chem*. 2019;27:116–124.
2 Townsend N, Wilson L, Bhatnagar P, et al. Cardiovascular disease in Europe 2016: an epidemiological update. *Eur Heart J*. 2016;37:3232–3245.
3 Lu Lu, Wu Z-Y, Li X, Han F. State-of-the-art: functional fluorescent probes for bioimaging and pharmacological research. *Acta Pharmacol Sin*. 2019;40:717–723.
4 Fuentes E, Moore-Carrasco R, de Andrade Paes AM, Trostchansky A. Role of Platelet Activation and Oxidative Stress in the Evolution of Myocardial Infarction. *J Cardiovasc Pharmacol Ther*. 2019;24:509–520.
5 Fan M, Han M, Xia Y, et al. Design and Synthesis of Potent PAR-1 Antagonists Based on Vorapaxar. *Bioorg Med Chem Lett*. 2020;30:127046. https://doi.org/10.1016/j.bmcl.2020.127046.
6 Celestini A, Violi F. A review of picotamide in the reduction of cardiovascular events in diabetic patients. *Vasc Health Risk Manag*. 2007;3:93–98.
7 Hennenberg M, Tamalunas A, Wang Y, et al. Inhibition of agonist-induced smooth muscle contraction by picotamide in the male human lower urinary tract outflow region. *Eur J Pharmacol*. 2017;803:39–47.
8 Sharma AN, Deyell JS, Sharma SN, Barseghian A. Role of and Recent Evidence for Antiplatelet Therapy in Prevention of Cardiovascular Disease in Diabetes. *Curr Cardiol Rep*. 2019;21. https://doi.org/10.1007/s11886-019-1168-y.
9 Xiu-jie L, Zhi-hao Z, Qing-song D, Xin C, Chao-qing W. Synthesis, in vitro cytotoxicity and anti-platelet activity of new 1,3-bentzenedisulfonamides. *Med Chem Res*. 2019;28:1864–1872.
10 Wang Y, Wang X, Chen X, et al. Synthesis and in vitro anti-platelet aggregation activities of 2-methoxy-5-arylamido-*N*-(pyridin-3-yl-methyl)benzamides. *Arch Pharm (Weinheim)*. 2019;352:1800257.
11 Wang CQ, Wang Y, Deng QS, et al. Synthesis of 4-Methoxy-1,3-Benzenediolylhydrazones and Evaluation of Their Anti-Platelet Aggregation Activity. *Iran J Pharm Res*. 2019;18:1803–1815.
12 Zhang Z-H, Wang X, Wang C-Q, Liu X-J. Synthesis, In Vitro Antiplatelet Activity of 4-Ethoxy-isophthalamides. *ChemistrySelect*. 2020;5:10163–10167.
13 Buccellati C, Sala A, Rossoni G, et al. Pharmacological characterization of 2NTX-99 [4- methoxy-N^1-(4-trans-nitrooxycyclohexyl)-N^3-(3-pyridinylmethyl)-1,3-benzenedicarboxamide], a potential antiatherothrombotic agent with antithromboxane and nitric oxide donor activity in platelet and vascular preparations. *J Pharmacol Exp Ther*. 2006;317:830–837.
14 Ma W-F, Yang H-K, Hu M-J, et al. One-pot synthesis and antiproliferative activity of novel 2,4-diaminopyrimidine derivatives bearing piperidine and piperazine moieties. *Eur J Med Chem*. 2014;84:127–134.
15 Sağlık BN, Osmaniye D, Çevik UA, et al. Synthesis, characterization and carbonic anhydrase I and II inhibitory evaluation of new sulfonamide derivatives bearing dithiocarbamate. *Eur J Med Chem*. 2020;198:112392. https://doi.org/10.1016/j.ejmech.2020.112392.
16 Liu X, Wang S, Zhang J, et al. Design, synthesis, and activities of novel derivatives of isophthalamide and benzene-1,3-disulfonamide. *Chem Res Chin U*. 2006;22:356–359.
17 Liu XJ, Shi XX, Zhong YL, Liu N, Liu K. Design, synthesis and in vitro activities on anti-platelet aggregation of 4-methoxybenzene-1,3-isophthalamides. *Bioorg Med Chem Lett*. 2012;22:6591–6595.
18 Liu X, Wang Y, Liu L, Chen G. Synthesis and in vitro activities on anti-platelet aggregation of 4-methoxyisophthalamides. *Med Chem Res*. 2018;27:1971–1983.
19 Chen G, Wang C, Zhang Z, Liu X. Synthesis and in vitro activities on anti-platelet aggregation of 4-methoxy-1,3-phthalamidesamides and benzenedisulfonamides. *Med Chem Res*. 2019;28:1413–1424.
20 Li GA, Wang X, Meng X, et al. Design, synthesis of novel *N*, *N*'-bis-(halogenophenyl)-4-methoxybenzene-1,3-disulfonamides and evaluation of their antiplatelet aggregation activity. *Acta Pharmaceutica Sinica*. 2015;50:185–190.
21 Chen X, Liu X, Qiu K, Xu X, Li C, Wang Y. *N*, *N*'-disubstitutedphenyl-4-ethoxyl benzene-1,3-disulfonamides: design, synthesis, and evaluation of anti-platelet aggregation activity. *Med Chem Res*. 2019;28:1388–1401.
22 Born GVR. Aggregation of blood platelets by adenosine diphosphate and its reversal. *Nature*. 1962;194:927–929.
23 Violi F, Ghiselli A, Iuliano L, et al. Inhibition bypicotamide of thromboxane production in vitro and ex vivo. *Eur J Clin Pharmacol*. 1988;33:599–602.
24 Abe S, Yamaguchi H, Ochi H, et al. Characteristic biological effects of itraconazole on L929 fibroblasts and their cell membrane. *J Infect Chemother*. 2000;6:35–40.
25 Xiong JW, Xiao H, Zhang ZX, Osumi M, Yamaguchi H. An experimental research on different detection conditions between MTT and CCK-8. *Acta Laser Biol Sin*. 2007;16:559–562.
26 Lipinski CA, Lombardo F, Dominy BW, et al. Experimental and computational approaches to estimate solubility and permeability in drug discovery and development settings. *Adv Drug Deliv Rev*. 2001;46:3–26.
27 Zhong F, Xing J, Li X, et al. (2018) Artificial intelligence in drug design. *Sci China Life Sci*. 2018;61:1191–1204.